Supplementary Information (SI) for Journal of Materials Chemistry A.

Environmentally responsible synthesis of high-performance P2-$Na_{2/3}[Ni_{1/3}Mn_{2/3}]O_2$ sodium-ion battery cathodes

Jintao Fu,[1] Mohamed H. Hassan,[1] Jiaxin Liu,[1] Hyeongjun Koh,[1] Alexander K. Ng,[1] Chiara Bruzzi,[1] John S. Corsi,[1] and Eric Detsi[1*]

[1]*Department of Materials Science & Engineering, University of Pennsylvania, Philadelphia, Pennsylvania 19104, USA*

** Corresponding author: ED detsi@seas.upenn.edu*

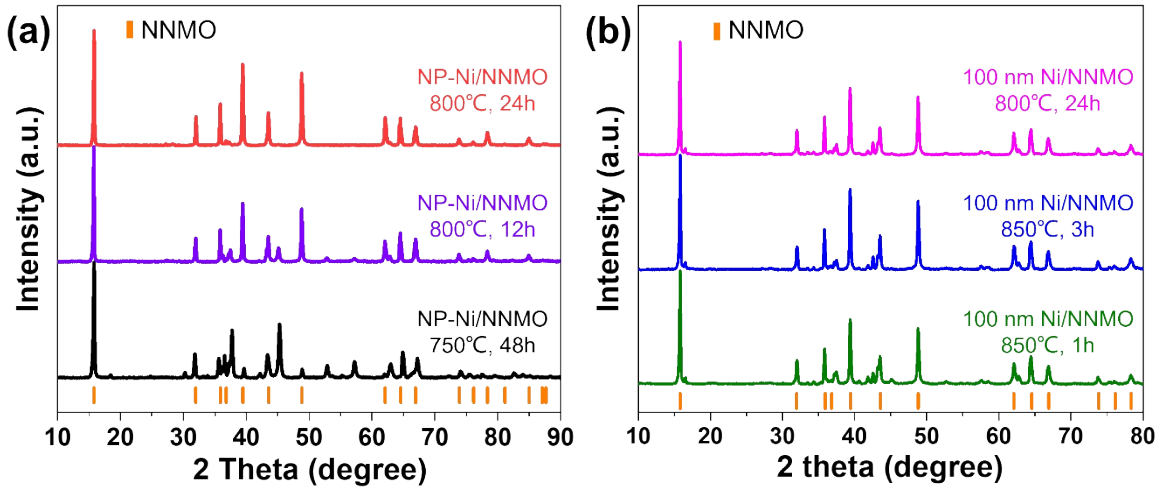

Figure S1. XRD profiles for NNMO converted from NP-Ni (a) and 100 nm Ni (b) under different annealing conditions. (a) For NP-Ni, the minimal requirement to yield full conversion is 24 h at 800 ℃, (red), since shorter annealing time (purple) or lower temperature (black) contained impurities. (b) For 100 nm Ni, NNMO conversion is mostly achieved with an annealing time as short as 1 h at 850 ℃ (green). However, the impurity peaks remained despite extending the annealing time (blue and magenta).

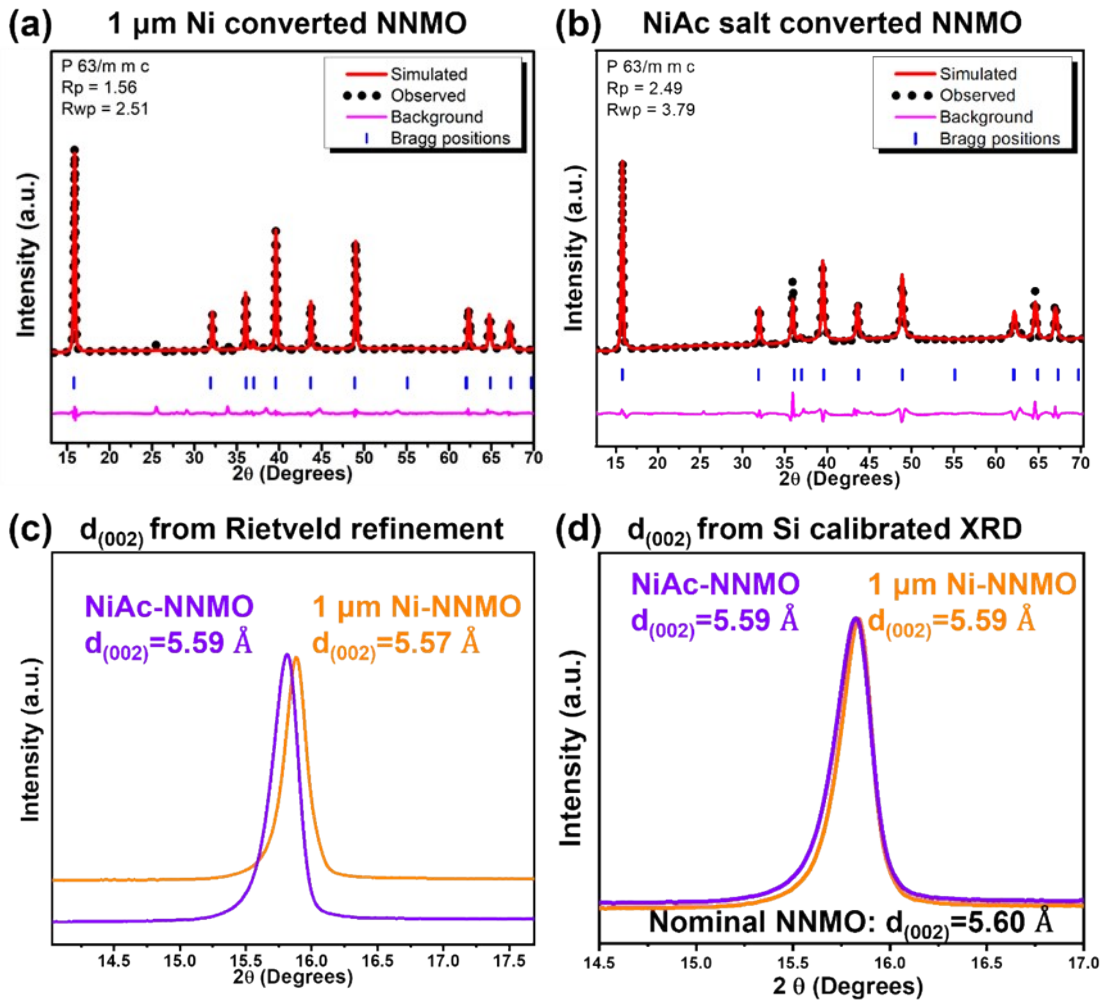

Figure S2. Rietveld refinement of (a) 1 µm Ni-NNMO and (b) NiAc-NNMO, with the corresponding $d_{(002)}$ spacing extracted from the refined results in (c). (d) $d_{(002)}$ spacing calculated from Si powder calibrated XRD. In both (c) and (d), the layer spacings are smaller than nominal value of 5.60 Å, which originates from the Na-rich composition.

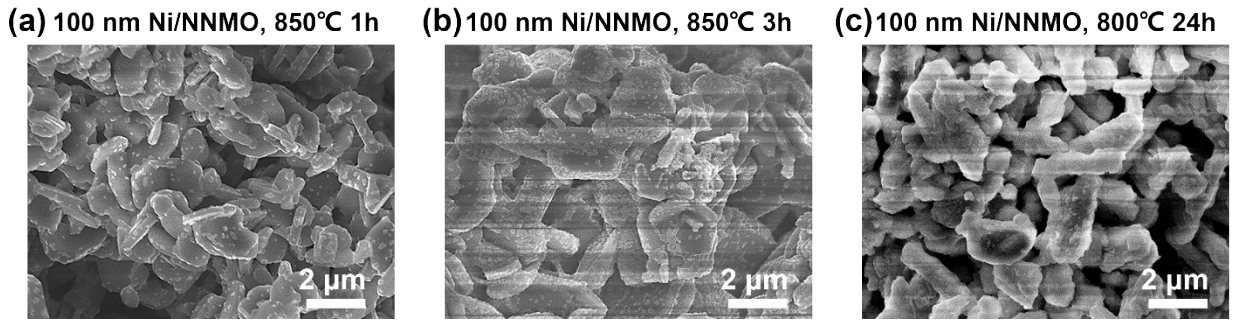

Figure S3. SEM images of NNMO converted from 100 nm Ni under different conditions. (a) Particles with a diameter of around 1 μm form after annealing for 1 h. (b-c) The particle size remains with extended annealing time.

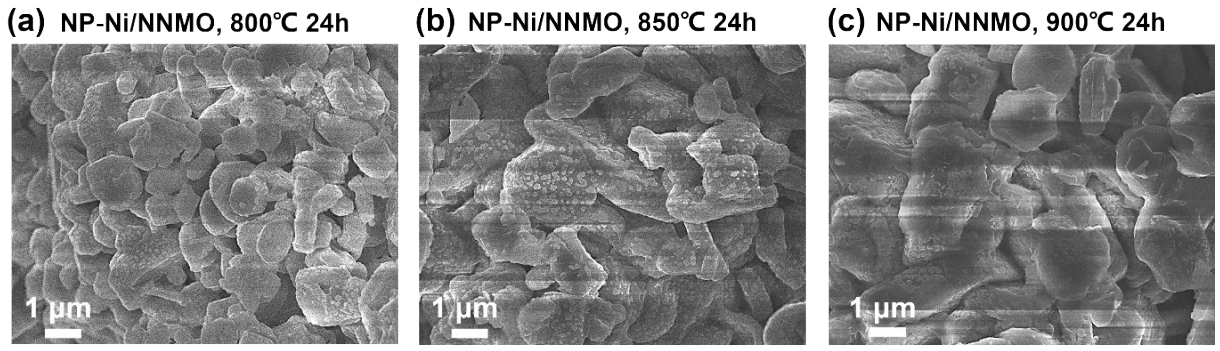

Figure S4. SEM images of NNMO converted from NP-Ni at different temperatures for 24 h. Particle coarsening is observed at higher temperature.

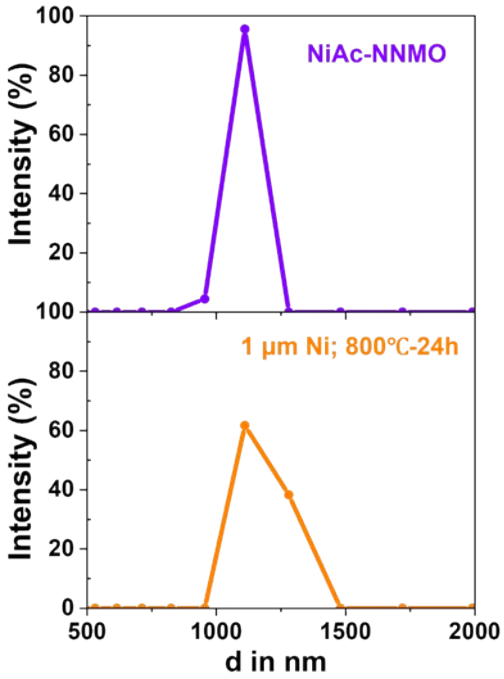

Figure S5. Dynamic light scattering (DLS) analysis of NiAc-NNMO (purple) and 1 µm Ni-NNMO (orange), revealing the average particle sizes in consistent with the SEM observations.

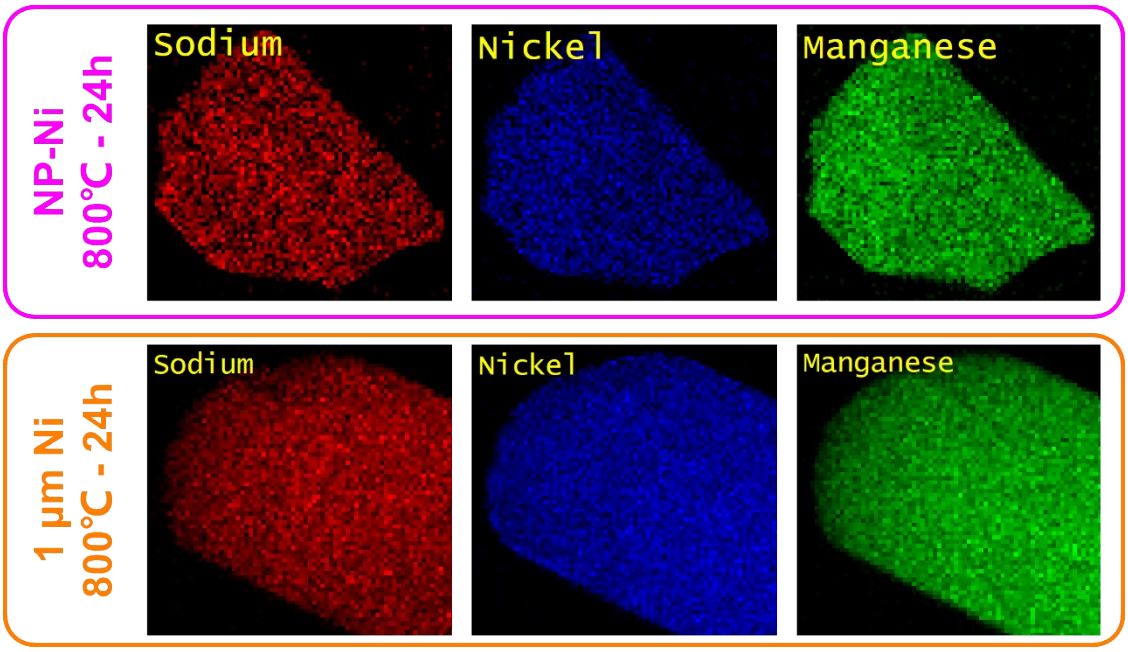

Figure S6. EDS maps of NNMO converted from NP-Ni (1st row) and 1 µm Ni (2nd row), confirming the homogeneous mixing of elemental Na, Ni, and Mn after conversion.

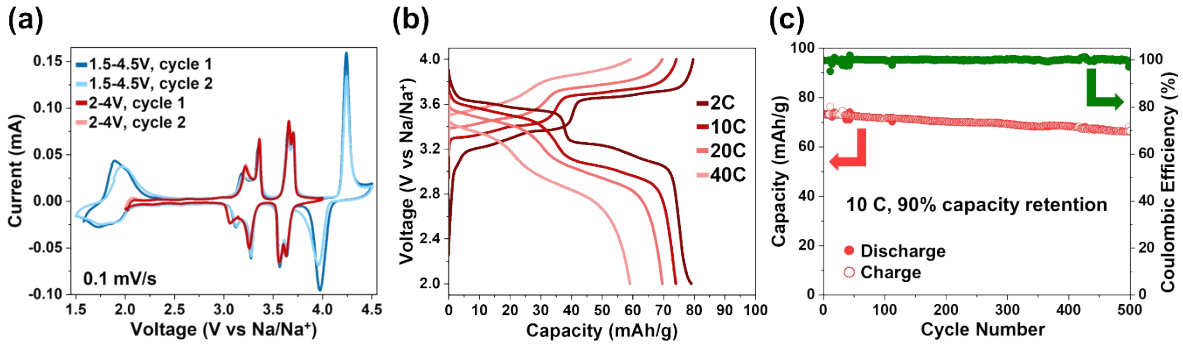

Figure S7. Cycling performance of NP-Ni converted NNMO as SIB cathode. (a) CV profile cycled between 2-4 V vs. Na/Na^+ (red) and ≈ 1.3-4.5 V vs. Na/Na^+ (blue). Decrease in peak intensity is observed for the latter case indicating structure change induced capacity decay. (b) Galvanostatic curves corresponding to the rate-capability test shown in **Figure 4b** in the main manuscript. (c) Long-term cycling at 10 C between 2-4 V vs. Na/Na^+. 90% capacity retention is achieved over 500 cycles.

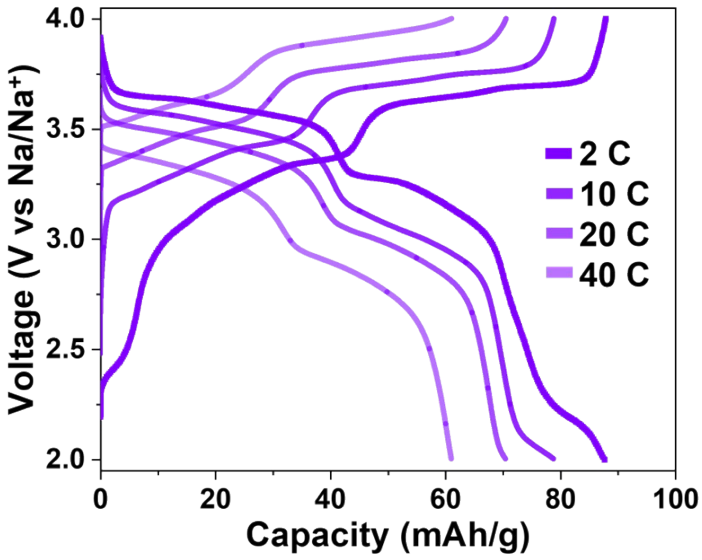

Figure S8. Galvanostatic curves of Ni acetate salt converted NNMO corresponding to the rate-capability test shown in **Figure 4b** in the main manuscript.

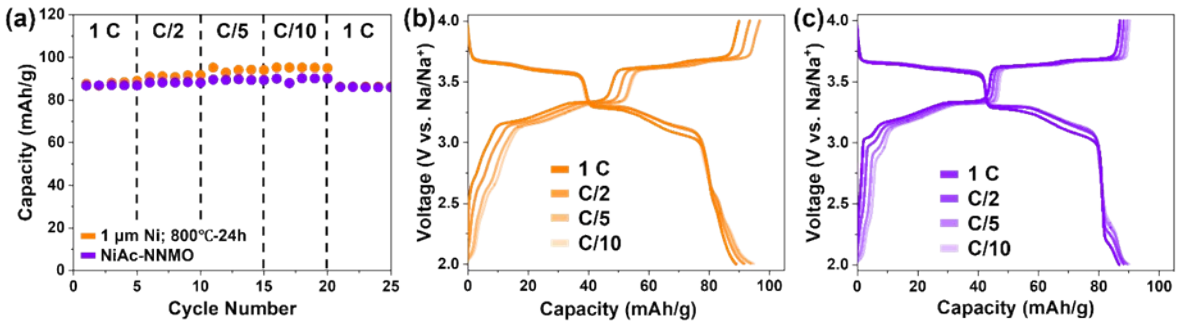

Figure S9. Rate-capability of NNMO converted from 1 μm Ni (orange) and Ni acetate salt (purple) cycled between 2-4 V vs. Na/Na^+, with the corresponding galvanostatic curves of 1 μm Ni-NNMO in (b) and NiAc-NNMO in (c).

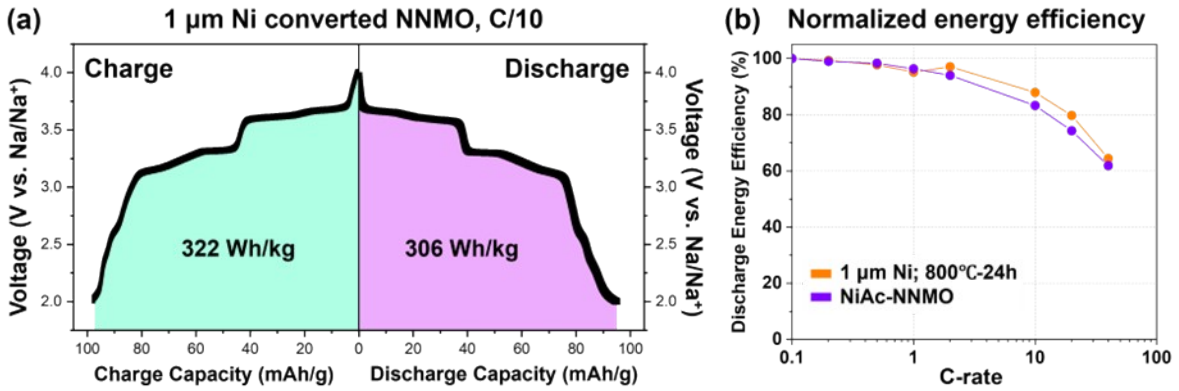

Figure S10. (a) Energy density of 1 μm Ni-NNMO at C/10 based on the E-Q profile. (b) Normalized energy efficiency against the slowest C-rate of C/10. Both 1 μm Ni-NNMO (orange) and NiAc-NNMO (purple) maintain >95% energy efficiency up to 1 C, and >60% energy efficiency at 40 C.

Kinetic analysis

Kinetic analysis is performed in the case of NP-Ni-NNMO to gain further insight into the reaction mechanism. **Figure S8a-b** shows the CV of NP-Ni-NNMO under different scan rates from 0.1 mV/s to

50 mV/s. The peak current (i) can be expressed as a function of scan rate (ν) as **Eq. 1**:[1,2]

$$i = a \cdot \nu^b \quad \textbf{(Eq. 1)}$$

where a and b are constants. The value of b varies between 0.5-1, with b=0.5 referring to a diffusion-controlled process (slow) and b=1 referring to a capacitive process (fast).[2] Taking logarithm on both sides of **Eq. 2**, an equivalent equation can be obtained:

$$\log(i) = \log(a) + b \cdot \log(\nu) \quad \textbf{(Eq. 2)}$$

Figure S11c shows such a log-log plot of peak current vs. scan rate, where the anodic and cathodic peak currents are taken from **Figure S11a-b** marked with "A" and "C", respectively. For scan rate up to 1 mV/s (corresponding to an equivalent C-rate of 0.9 C), the b-values for both the anodic and cathodic process were above 0.8, indicating the Na insertion/extraction behavior is more similar to a capacitor. For scan rates 1-10 mV/s (corresponding to an equivalent C-rate of 0.9-9 C), the b-values dropped to ~0.7, suggesting the onset of diffusion-controlled kinetics,[2] while this value is still higher than other P2-NNMO (0.5-0.6).[3] Thus, our kinetic analysis result is consistent with the observed high rate-capability.

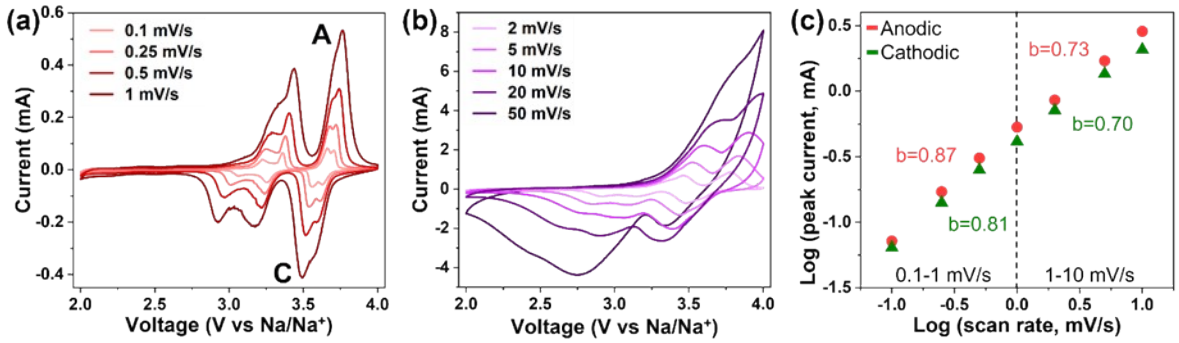

Figure S11. (a-b) Cyclic voltammetry of NP-Ni converted NNMO at different scan rates. (c) The linear relationship between peak current and scan rate in a log-log plot to obtain the b-values.

References:

1 H. Lindström, S. Södergren, A. Solbrand, H. Rensmo, J. Hjelm, A. Hagfeldt and S.-E. Lindquist, J Phys Chem B, 1997, 101, 7717–7722.

2 B. K. Lesel, J. S. Ko, B. Dunn and S. H. Tolbert, ACS Nano, 2016, 10, 7572–7581.

3 Y. Liu, Q. Shen, X. Zhao, J. Zhang, X. Liu, T. Wang, N. Zhang, L. Jiao, J. Chen and L.-Z. Fan, Adv Funct Mater, 2020, 30, 1907837.